Electronic band structure of wurtzite GaN under biaxial strain in the *M* plane investigated with photoreflectance spectroscopy

Sandip Ghosh, P. Waltereit, O. Brandt, H. T. Grahn,* and K. H. Ploog
Paul-Drude-Institut für Festkörperelektronik, Hausvogteiplatz 5–7, 10117 Berlin, Germany
(Received 25 August 2001; published 7 January 2002)

We investigate the modification of the electronic band structure in wurtzite GaN due to biaxial strain within the *M* plane using photoreflectance (PR) spectroscopy. The compressively strained *M*-plane GaN film is grown on γ-$LiAlO_2$ (100). In the PR measurements, the electric-field vector (**E**) of the probe light is polarized parallel ($\|$) and perpendicular ($\perp$) to the **c** axis of GaN which lies in the growth plane. For $\mathbf{E}\perp\mathbf{c}$, the spectrum exhibits only a single resonant feature at lower energies, while for $\mathbf{E}\|\mathbf{c}$ a different single resonant feature appears at higher energies. To identify these features, we calculate the strain dependence of the interband transition energies and the components of the oscillator strength using the $\mathbf{k}\cdot\mathbf{p}$ perturbation approach. Comparison with the calculations shows that the origin of the PR features and their significant in-plane polarization anisotropy is related to the influence of *M*-plane, biaxial compressive strain on the valence-band structure of GaN. We estimate the value of the deformation potential D_5 to be -4.7 eV.

DOI: 10.1103/PhysRevB.65.075202 PACS number(s): 71.20.Nr, 71.70.Fk, 78.66.Fd, 78.40.Fy

I. INTRODUCTION

The wurtzite (WZ) structure of III-V nitrides leads to electrostatic fields due to spontaneous and piezoelectric polarization, when the film growth is along the [0001] direction, i.e., for *C*-plane-oriented films.[1] These electrostatic fields separate the electron and hole envelope wave functions in a heterostructure such as a quantum well. The consequent reduction in the envelope wave-function overlap results in a lower radiative efficiency for light-emitting devices.[2] A way to overcome this problem is to grow films along nonpolar directions such as $[1\bar{1}00]$, i.e., *M*-plane-oriented films. The growth of *M*-plane GaN films has been a challenge due to the lack of substrates that favor such orientation during film growth. Recently, the growth of *M*-plane-oriented films on γ-$LiAlO_2$ (100) substrates was demonstrated.[3] It was experimentally shown that the electrostatic fields can be avoided in such nitride quantum wells.[4] However, the lattice mismatch between the film and the substrate results in in-plane strain, which can strongly influence the electronic band structure (EBS) of the material.

EBS modification due to biaxial strain in the *C* plane (*x*-*y* plane) of WZ-GaN has been studied extensively both theoretically and experimentally.[5] Isotropic strain in the *C* plane (with strain components $\epsilon_{xx}=\epsilon_{yy}$) preserves the symmetry in the *x*-*y* plane of the WZ-GaN lattice so that no significant in-plane optical polarization anisotropy occurs. For anisotropic strain in the *C* plane, an in-plane polarization anisotropy can arise, which has been confirmed experimentally.[6] The situation is expected to be quite different for an *M*-plane sample, where the unique **c** axis lies within the growth plane. Here, even in the absence of in-plane strain, one expects to see an in-plane polarization anisotropy. Any biaxial strain within the *M* plane (*x*-*z* plane) further lifts the symmetry in the *x*-*y* plane of the WZ-GaN lattice. According to theoretical predictions,[7,8] biaxial strain within the *M* plane would significantly modify the top two valence-band (VB) states. While in the absence of any strain these VB states have wave functions with nearly identical symmetry, this is no longer true in the presence of biaxial strain in the *M* plane. This change in symmetry affects the polarization selection rules for interband transitions. Therefore, additional changes are expected in the polarization properties of an *M*-plane GaN film due to in-plane strain. However, to the best of our knowledge, so far there exists no direct experimental evidence for the EBS modification and the consequent changes in the optical polarization properties of GaN due to biaxial strain in the *M* plane.

In this paper, we use photoreflectance (PR) spectroscopy to study the EBS modification of an *M*-plane GaN film due to in-plane biaxial compressive strain. The resonant features observed in the PR spectrum have different energies from those expected for unstrained GaN and show strong in-plane polarization anisotropy. We perform a $\mathbf{k}\cdot\mathbf{p}$ perturbation-based EBS calculation and determine the strain dependence of the energy of the three interband transitions at the fundamental band gap of GaN as well as the components of their oscillator strength. By comparison with the calculated EBS results, we identify the origin of the PR features and explain their polarization properties.

The paper is organized in the following way. In Sec. II, we present the sample structure and the PR setup. In Sec. III, we describe in detail the EBS calculation. In Sec. IV, we present the experimental results. The comparison of the experimental results with the EBS calculations and a discussion of the results are presented in Sec. V. Finally, we give a brief summary of the investigation in Sec. VI.

II. EXPERIMENTAL DETAILS

The *M*-plane GaN film (1.22 μm thick) used in this study was grown by rf plasma-assisted molecular-beam epitaxy (MBE) on a γ-$LiAlO_2$(100) substrate.[3] High-resolution triple-axis x-ray diffraction (XRD) and Raman spectroscopy were used to verify the *M*-plane orientation of the film and its single phase nature (i.e., absence of *C*-plane-oriented domains).[3] Figure 1 shows the XRD profile across the $(1\bar{1}00)$

 ©2002 The American Physical Society

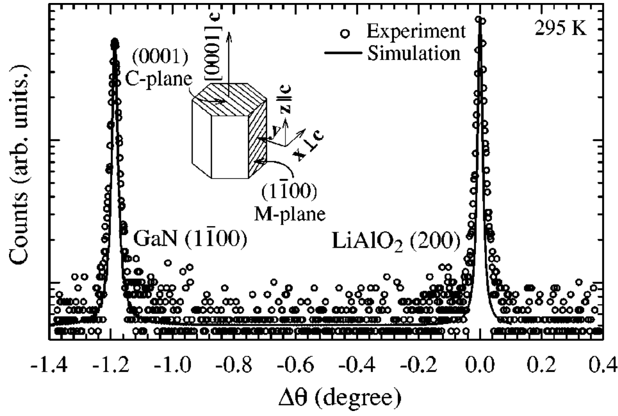

FIG. 1. Experimental and simulated triple-axis x-ray θ-2θ scan across the symmetric (1$\bar{1}$00) reflection of the M plane GaN film on $LiAlO_2$(100) substrate. The inset shows the wurtzite GaN unit cell and the choice of coordinates.

reflection of the sample. The inset displays the wurtzite-GaN unit cell and the choice of coordinates. The angular position of the (1$\bar{1}$00) reflection corresponds to a biaxial compressive strain in the M-plane with an out-of-plane dilatation $\epsilon_{yy}=0.29\%$. This result is in agreement with Raman measurements, which exhibit strongly blueshifted lines. Note that compressive strain is to be expected both from the lattice mismatch (-0.3% along **z**, -1.7% along **x**) between GaN(1$\bar{1}$00) and $LiAlO_2$(100) and from the thermal mismatch, which is compressive along both directions as well. For comparison, a C-plane GaN film, which is not expected to show any in-plane polarization anisotropy, was also studied to rule out spurious sources of polarization anisotropy. This C-plane GaN film was grown by reactive MBE on a 6H-SiC (0001) substrate[9] and is under biaxial tensile strain with an out-of-plane contraction $\epsilon_{zz}=-0.08\%$.

Modulation spectroscopy techniques such as PR are usually the preferred method for the study of the EBS of semiconductors.[10] The PR technique is relatively insensitive to defects, has high-temperature capability, and reveals transitions at energies higher than the fundamental gap. In the PR measurements, we used a He-Cd laser (3.815 eV) as the pump beam. The probe beam (angle of incidence $\sim 10°$) was obtained by dispersing the output of a Xe lamp using a 0.64 m monochromator (energy-band pass $\sim$4 meV) and linearly polarizing the output beam with a Glan-Taylor prism. The electric-field vector (**E**) of the probe beam was usually polarized parallel (∥) or perpendicular (⊥) to the **c** axis. A second 1.0 m monochromator running synchronously with the first was used as a narrow-band pass filter in front of the UV-enhanced silicon detector. This setup helps to reduce the background signal and noise arising from the scattered pump beam and photoluminescence (PL) emission at low temperatures. Phase sensitive detection was performed using a lock-in amplifier.

III. ELECTRONIC BAND-STRUCTURE CALCULATIONS

In unstrained WZ-GaN, there are three closely spaced top VB's at the Brillouin-zone center (wave vector $\mathbf{k}=0$), Γ_9, Γ_7^{upper}, and Γ_7^{lower} labeled here as heavy hole (HH), light hole (LH), and spin-orbit crystal-field split-off hole (SCH), respectively. The excitons involving electrons in the conduction band (CB) and holes in the HH, LH, and SCH bands are referred to as A, B, and C excitons, respectively. The states at the CB bottom have atomic s orbital character. The top HH and LH band states have essentially atomic p_x and p_y orbital character (wave function $|X\pm iY\rangle$-like), while the SCH band states have p_z orbital character (wave function $|Z\rangle$-like). The **c** axis defines the **z** direction. Due to strain, the VB states are strongly modified affecting both the energies as well as the polarization selection rules for the transitions. To theoretically estimate the strain-induced EBS modification at $\mathbf{k}=0$, we adopt the $\mathbf{k}\cdot\mathbf{p}$ perturbation approach outlined by Bir and Pikus.[11] Since the large band gap of GaN reduces the interaction between the VB and the CB states,[12] the Hamiltonian for the strain dependence of the VB can be separately given by the following 6×6 matrix:

$$H^v=\begin{bmatrix} F & 0 & -H^* & 0 & K^* & 0 \\ 0 & G & \Delta & -H^* & 0 & K^* \\ -H & \Delta & \lambda & 0 & I^* & 0 \\ 0 & -H & 0 & \lambda & \Delta & I^* \\ K & 0 & I & \Delta & G & 0 \\ 0 & K & 0 & I & 0 & F \end{bmatrix},$$

where

$$F=\Delta_1+\Delta_2+\lambda+\theta, \quad G=\Delta_1-\Delta_2+\lambda+\theta,$$

$$H=i(A_6k_zk_+ + A_7k_+ + D_6\epsilon_{z+}),$$

$$I=i(A_6k_zk_+ - A_7k_+ + D_6\epsilon_{z+}),$$

$$K=A_5k_+^2+D_5\epsilon_+, \quad \Delta=\sqrt{2}\Delta_3,$$

$$\lambda=A_1k_z^2+A_2k_\perp^2+D_1\epsilon_{zz}+D_2(\epsilon_{xx}+\epsilon_{yy}),$$

$$\theta=A_3k_z^2+A_4k_\perp^2+D_3\epsilon_{zz}+D_4(\epsilon_{xx}+\epsilon_{yy}),$$

$$\epsilon_+=\epsilon_{xx}-\epsilon_{yy}+2i\epsilon_{xy}, \quad \epsilon_{z+}=\epsilon_{xz}+i\epsilon_{yz},$$

$$k_+=k_x+ik_y, \quad k_\perp^2=k_x^2+k_y^2. \tag{1}$$

The parameters D_j ($j=1$ to 6) denote the deformation potentials for the VB, and A_j ($j=1$ to 7) are equivalent to the Luttinger parameters and determine the hole effective masses. ϵ_{lm} and k_l ($l,m=x,y,z$) are the strain and wave-vector components, respectively. Δ_1 is the crystal-field energy parameter, while Δ_2 and Δ_3 are spin-orbit energy parameters. The basis functions used to obtain H^v are $(1/\sqrt{2})|X+iY,\alpha\rangle$, $(1/\sqrt{2})|X+iY,\beta\rangle$, $|Z,\alpha\rangle$, $|Z,\beta\rangle$, $(1/\sqrt{2})|X-iY,\alpha\rangle$, and $(1/\sqrt{2})|X-iY,\beta\rangle$. Here $|X\rangle$, $|Y\rangle$, and $|Z\rangle$ have symmetry properties of the atomic p_x, p_y, and p_z orbital functions under the operations of the C_{6v}^4 group. $|\alpha\rangle$ and $|\beta\rangle$ denote the spin-wave functions corresponding to spin up and spin down. The diagonalization of the above matrix yields three distinct VB maxima with energies E_j^v.

The Hamiltonian for the strain dependence of the CB minimum is given by a diagonal 2×2 matrix with basis functions $|S,\alpha\rangle$ and $|S,\beta\rangle$. Its single distinct eigenvalue can be expressed as

$$E^c=\alpha_{\parallel}\epsilon_{zz}+\alpha_{\perp}(\epsilon_{xx}+\epsilon_{yy})+\frac{\hbar^2k_z^2}{2m_{\parallel}^e}+\frac{\hbar^2k_{\perp}^2}{2m_{\perp}^e}, \quad (2)$$

where α and m^e denote the CB deformation potential and the electron effective mass, respectively. The excitonic transition energies are then given by

$$E_j=E^*+E^c-E_j^v-E_{ex}^b, \quad (3)$$

where $E^*=E_g+\Delta_1+\Delta_2=3.532$ eV. The band gap E_g was chosen such that the A-exciton transition energy in unstrained GaN is 3.479 eV in the low-temperature limit as observed in experiments on free standing GaN.[13] E_{ex}^b denotes the exciton binding energy and is taken to be 26 meV for all three transitions.

The components of the oscillator strengths for the transitions, which determine the polarization selection rules, are obtained from momentum matrix elements of the type $|\langle\Psi^{CB}|p_l|\Psi^{VB}\rangle|^2$ with $l=x,y,z$. Here, $\langle\Psi^{CB}|=\langle S|$ and $|\Psi^{VB}\rangle=a_1|X\rangle+a_2|Y\rangle+a_3|Z\rangle$ represent the orbital part of the CB and VB basis functions, respectively. The coefficients a_j are obtained by determining the eigenvectors of H^v. The relative values of $|\langle S|p_x|X\rangle|^2$, $|\langle S|p_y|Y\rangle|^2$, and $|\langle S|p_z|Z\rangle|^2$ were taken to be equal, in accordance with earlier theoretical results.[14]

The relation between the in-plane and the out-of-plane strain components, which are needed for the calculations, can be obtained as follows. An M-plane film, under in-plane biaxial strain, is free to expand or contract in the out-of-plane direction. This implies that the out-of-plane stress component $\sigma_{yy}=0$ and leads to the following relation between the strain components:

$$\epsilon_{yy}=-\frac{C_{12}}{C_{11}}\epsilon_{xx}-\frac{C_{13}}{C_{11}}\epsilon_{zz}, \quad \epsilon_{xy}=\epsilon_{yz}=\epsilon_{zx}=0, \quad (4)$$

where C_{ij} are the elastic stiffness constants.[15]

Since we are interested in the transition energies only at $\mathbf{k}=0$, the number of required parameters (α, D_1 to D_5, Δ_i) is actually smaller. We estimate the required parameters by combining two previously reported experimental and theoretical results of strain dependent studies on C-plane GaN as follows. For GaN under isotropic biaxial strain in the C plane, it is possible to write a simplified analytical expression for the strain dependence of the three excitonic transition energies. Fitting these expressions to a set of experimental data, Shikanai *et al.*[16] estimated $\Delta_1=22$ meV, $\Delta_2=5$ meV, and derived the following relations:

$$\Xi-\left(D_1-\frac{C_{33}}{C_{13}}D_2\right)=38.9 \text{ eV}, \quad (5a)$$

$$\left(D_3-\frac{C_{33}}{C_{13}}D_4\right)=23.6 \text{ eV}. \quad (5b)$$

Ξ denotes the combined dilatational component of the deformation potential acting on the CB, which for a C-plane sample with $\epsilon_{xx}=\epsilon_{yy}$ can be expressed as

$$\Xi=\alpha_{\parallel}-\frac{C_{33}}{C_{13}}\alpha_{\perp}. \quad (6)$$

The local atomic coordination of the WZ structure is the same as that for the cubic zinc-blende structure and differs only for the relative positions of the third-nearest neighbors and beyond. This justifies a quasicubic approximation,[11] which relates some of the required parameters to each other and has been verified by first-principles EBS calculations.[12] Of interest to us here are the relations

$$2D_4=-D_3, \quad (7a)$$

$$D_1-D_2=-D_3, \quad (7b)$$

$$\alpha_{\parallel}=\alpha_{\perp}=\alpha, \quad (7c)$$

$$\Delta_3=\Delta_2. \quad (7d)$$

Using Eq. (5b) and Eq. (7a), we can determine D_3 and D_4.

To determine D_1, D_2, and D_5, different assumptions have been made previously.[7,17] Shikanai *et al.*[16] found that their experimentally determined D_3^{exp} and D_4^{exp} values differed from the theoretically estimated values D_3^{theory} and D_4^{theory} of Suzuki and Uenoyama.[5,18] Both ratios D_3^{exp}/D_3^{theory} and D_4^{exp}/D_4^{theory} have a value of about 2.7. We obtain D_1 and D_2 by multiplying the values of these parameters as obtained by Suzuki and Uenoyama by a factor of 2.7. In this way, Eq. (7b) continues to be satisfied as were Suzuki and Uenoyama original values. The initial value of D_5 is also obtained in this fashion, and then slightly adjusted ($\sim$15%) to fit our experimental results. Finally, we estimate α by combining Eq. (5a), Eq. (6), Eq. (7c), and the D_j values. The deformation-potential parameter values thus obtained are $\alpha_{\perp}=\alpha_{\parallel}=\alpha=-44.5$ eV, $D_1=-41.4$ eV, $D_2=-33.3$ eV, $D_3=8.2$ eV, $D_4=-4.1$ eV, and $D_5=-4.7$ eV. The resulting interband hydrostatic deformation potentials $\alpha-D_1=-3.1$ eV and $\alpha-D_2=-11.2$ eV are comparable in magnitude to previously reported values listed in Refs. 5 and 19. The above parameters reproduce very well the experimentally observed EBS modification of GaN under isotropic biaxial C-plane strain as reported by Shikanai *et al.*[16] Two earlier experimental studies[6,20] on C-plane GaN with anisotropic in-plane strain had reported D_5 values to be -2.4 eV and -3.3 eV, while the closest theoretical estimate[21] for its value is -4.0 eV.

M-plane strain leads to significant changes in the original VB states so that it is no longer possible to describe the transitions in terms of A-, B-, and C-exciton transitions of unstrained GaN. We have adopted the nomenclature E_1, E_2, and E_3 for the three ($n=1$) exciton transitions representing increasing energy. Figure 2(a) shows the variation of these three calculated transition energies with isotropic biaxial M-plane strain ($\epsilon_{xx}=\epsilon_{zz}$). The dashed lines reveal two anticrossings. Figures 2(b)–2(d) show the x, y, and z components of the oscillator strengths of the three transitions. These re-

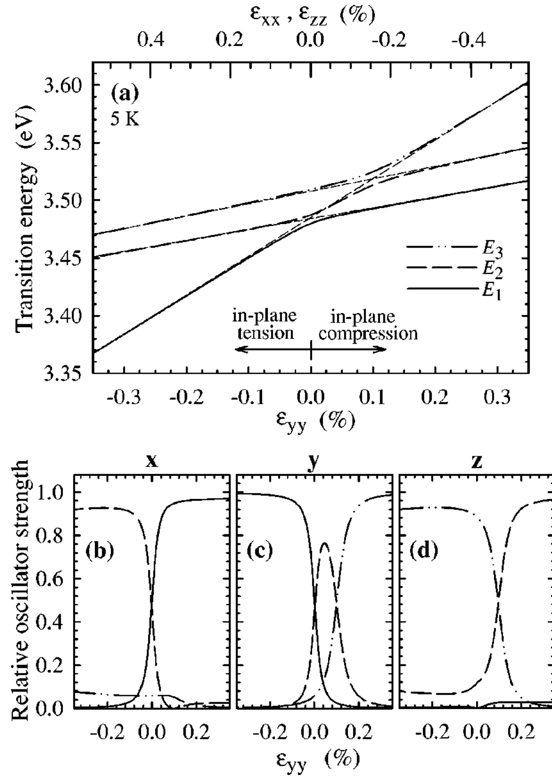

FIG. 2. (a) Calculated E_1, E_2, and E_3 exciton transition energies as a function of isotropic biaxial strain ($\epsilon_{xx}=\epsilon_{zz}$) in the *M* plane of WZ-GaN. The thin dashed lines indicate two anticrossings. (b)–(d) Relative *x*, *y*, and *z* components of the oscillator strength for the E_1, E_2, and E_3 transitions as a function of isotropic biaxial strain in the *M* plane of WZ-GaN.

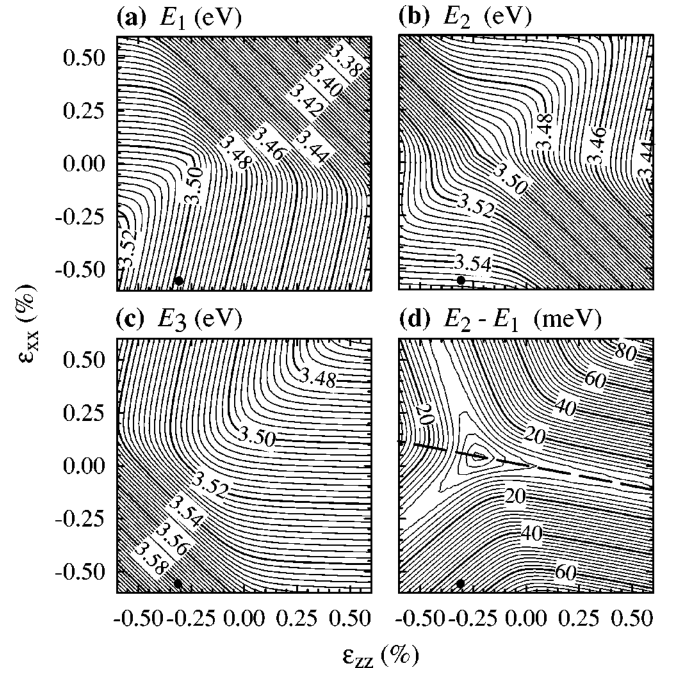

FIG. 3. Calculated (a) E_1, (b) E_2, and (c) E_3 transition energies as a function of in-plane strain ϵ_{xx} and ϵ_{zz} for an *M*-plane GaN film at 5 K. (d) Energy difference E_2-E_1 as a function of in-plane strain ϵ_{xx} and ϵ_{zz}. The dashed line represents the trajectory $\epsilon_{xx}=-0.1833\epsilon_{zz}$. The black spots mark the in-plane strain $\epsilon_{xx}=-0.56\%$ and $\epsilon_{zz}=-0.31\%$, for which the calculated E_1 and E_2 transition energies coincide with the ones measured by PR.

sults suggest that for large isotropic in-plane compressive strain the E_1 transition is predominantly *x* polarized, E_2 *z* polarized, while E_3 is *y* polarized. For large in-plane tensile strain, the E_1 transition becomes predominantly *y* polarized, E_2 *x* polarized, while E_3 becomes *z* polarized. These polarization properties arise essentially from the symmetry of the wave functions of strain-modified VB edge states. *M*-plane strain lifts the symmetry in the *x*-*y* plane of the wurtzite crystal and separates the original $|X\pm iY\rangle$-like HH and LH states of unstrained WZ-GaN to $|X\rangle$-like and $|Y\rangle$-like states. A compressive strain along **x** induces a dilatation along **y** so that the energy of the $|X\rangle$-like state is raised, while that of the $|Y\rangle$-like state is lowered. Therefore, the energy for the interband transition between the CB and the $|X\rangle$-like VB is lower compared to that between the CB and the $|Y\rangle$-like VB. The situation is reversed for tensile stress along **x**, where the energy for the interband transition between the CB and the $|Y\rangle$-like VB is lower. While a *C*-plane GaN film with isotropic in-plane strain does not exhibit any in-plane polarization anisotropy,[22,23] an *M*-plane GaN film with isotropic in-plane strain continues to show a significant in-plane polarization anisotropy. These calculated polarization characteristics are in general agreement with two earlier predictions in Refs. 7 and 8, where only relative shifts between the VB states were calculated (i.e., setting D_1 and $D_2=0$). Here, we estimate the absolute transition energies for direct comparison with experiments by determining all relevant deformation potentials.

The *C*-plane GaN films are mostly grown on substrates with similar hexagonal symmetry, which leads to isotropic in-plane strain ($\epsilon_{xx}=\epsilon_{zz}$). However, due to the inherent lower symmetry of the *M* plane, a GaN film with an *M*-plane orientation is likely to experience anisotropic in-plane strain. We therefore extended our calculation to arbitrary in-plane strain in the range $|\epsilon_{xx}|$ and $|\epsilon_{zz}|\leqslant 0.6\%$. The variation of the E_1, E_2, and E_3 transition energies with in-plane strain is shown by the contour plots in Figs. 3(a)–3(c). Figure 3(d) displays the difference E_1-E_2. For $\epsilon_{xx}\sim 0.04\%$ and $\epsilon_{zz}\sim -0.24\%$, the difference $E_1-E_2\sim 0$. By comparison with a similar calculation for *C*-plane strain (not shown here), we identify this strain coordinate to correspond to a zinc-blende-like situation, where the in-plane strain counteracts the crystal-field splitting such that the top two VB states are degenerate at $\mathbf{k}=0$. Therefore, for example, with a strain variation along $\epsilon_{xx}=-0.1833\epsilon_{zz}$ [dashed line in Fig. 3(d)], we will encounter only one apparent anticrossing between the three transition energies, just as in the case of *C*-plane strain with $\epsilon_{xx}=\epsilon_{yy}$.[16,22]

The relative values of the *x*, *y*, and *z* components of the oscillator strengths for the three transitions are shown by the gray-scale contour plots in Fig. 4 for *M*-plane strain in the range $|\epsilon_{xx}|$ and $|\epsilon_{zz}|\leqslant 0.6\%$. For future reference, we note that these plots show that for ϵ_{xx} and $\epsilon_{zz}\lesssim -0.2\%$, the E_1,

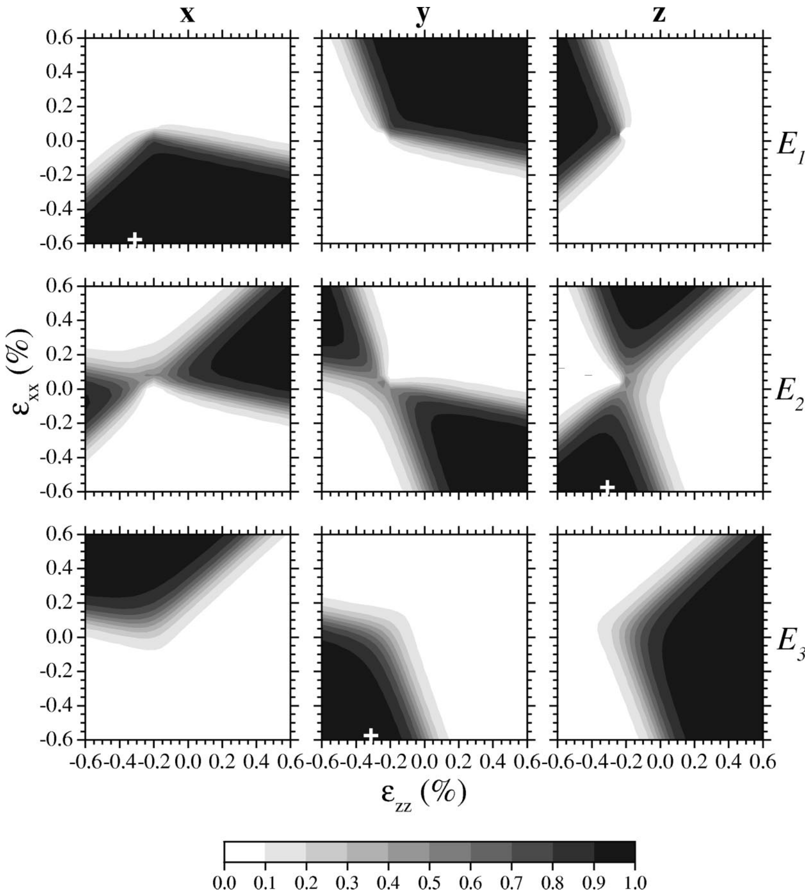

FIG. 4. Relative x, y, and z components of the oscillator strength of the E_1, E_2, and E_3 transitions as a function of in-plane strain ϵ_{xx} and ϵ_{zz} for an M-plane GaN film. The white crosses indicate the predominant polarization for the E_1, E_2, and E_3 transitions for the in-plane strain $\epsilon_{xx}=-0.56\%$ and $\epsilon_{zz}=-0.31\%$.

E_2, and E_3 transitions are predominantly x polarized, z polarized, and y polarized, respectively.

IV. EXPERIMENTAL RESULTS

Figure 5(a) shows the PR spectra of the M-plane sample for $\mathbf{E}\perp\mathbf{c}$ and $\mathbf{E}\|\mathbf{c}$ recorded at 295 and 5 K. The schematic inset shows the measurement geometry, with ϕ being the in-plane polarization angle relative to the **c** axis. When the polarization of the light is rotated by 90° from $\mathbf{E}\perp\mathbf{c}$ (i.e., $\mathbf{E}\|\mathbf{x}$, $\phi=90°$) to $\mathbf{E}\|\mathbf{c}$ (i.e., $\mathbf{E}\|\mathbf{z}$, $\phi=0°$) in the M plane, we find that the spectrum is shifted to higher energies. For each polarization, the spectrum consists of a single resonant feature. To determine the corresponding transition energy, we fit these features by Aspnes' line-shape function with redefined parameters,[24,25]

$$\frac{\Delta R}{R}(E)=\mathrm{Re}\left[\frac{a\kappa_2(\kappa_1\gamma)^m e^{i(\delta+[m-3]\pi/2)}}{(E-E_j+i\kappa_1\gamma)^m}\right]. \qquad (8)$$

With the exponent $m=3$, the generalized Lorentzian function above mimics the first derivative Gaussian-broadened excitonic transition line shape.[26] The fitting parameters E_j, γ, a, and δ denote the transition energy, broadening parameter, amplitude, and phase factor, respectively. $\kappa_1=0.364m-0.147$ and $\kappa_2=-0.115m+1.7$ are constants. The transition energies obtained from fitting are 3.428 eV (3.498 eV) for $\mathbf{E}\perp\mathbf{c}$ and 3.468 eV (3.546 eV) for $\mathbf{E}\|\mathbf{c}$ at 295 K (5 K). The error is 3 meV for all values. Thus, the effective band gap of the M-plane film increases by 40 meV (48 meV) at 295 K (5 K), when the in-plane polarization of the probe light is rotated by 90° from $\mathbf{E}\perp\mathbf{c}$ to $\mathbf{E}\|\mathbf{c}$.

Since the PR spectrum of the M-plane sample depends critically on the polarization angle ϕ, we have to verify that the angular alignment is correct. If the spectra shown in Fig. 5(a) are indeed for properly aligned $\mathbf{E}\|\mathbf{c}$ and $\mathbf{E}\perp\mathbf{c}$ situations, they represent the only two possible independent line shapes. Therefore, for any other ϕ, the line shape can be approximated by a linear combination of the type

$$\frac{\Delta R}{R}(E,\phi)=\frac{\Delta R_\|}{R_\|}(E)\cos^2(\phi)+\frac{\Delta R_\perp}{R_\perp}(E)\sin^2(\phi), \qquad (9)$$

where $\Delta R_\|/R_\|$ ($\Delta R_\perp/R_\perp$) represents the line shape measured for $\phi=0°$ ($\phi=90°$) with the assumption $R_\|\sim R_\perp$. To test this, we fix the probe beam energy at 3.45 eV (295 K), where $\Delta R_\|/R_\|=2.3\times10^{-4}$ and $\Delta R_\perp/R_\perp=-2.25\times10^{-4}$. We then calculate the signal strength for any other ϕ using Eq. (9). The circles in Fig. 5(b) show a polar plot of the measured $|\Delta R/R|$, which agrees very well with the calculated variation shown by the solid line. This angular dependence of the PR signal also demonstrates the lower symmetry (twofold rotation) of the M-plane GaN film.

To rule out the possibility that these polarization characteristics arise from other sources, we studied a C-plane GaN sample, where we did not find any significant in-plane polarization anisotropy as expected. Normally, when PR measurements are used for characterization of III-V semiconductors

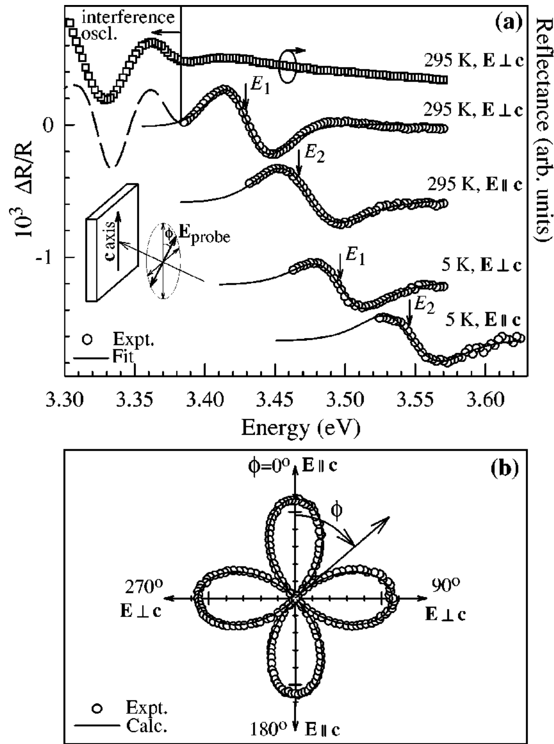

FIG. 5. (a) Experimental PR spectra (circles) of the *M*-plane GaN film for different polarizations of the probe beam relative to the **c** axis of GaN. The schematic inset shows the measurement geometry. The plots are vertically displaced for clarity. The solid lines are fits using Eq. (8) extrapolated to lower energies. The vertical arrows indicate the transition energies. Optical interference-related features in the PR spectra at lower energies (dashed line) were not included in the energy range for fitting. They were identified by comparison with the corresponding *R* spectra, an example of which is shown for $\mathbf{E}\perp\mathbf{c}$ at the top (squares). (b) Polar plot of the measured PR signal magnitude (circles) at 3.45 eV (295 K) as a function of the in-plane polarization angle ϕ of the probe beam relative to the **c** axis. The major tick on the vertical and horizontal axes corresponds to $|\Delta R/R|=2\times10^{-4}$. The lines represent the calculated variation based on Eq. (9).

and alloys with (001) zinc-blende or *C*-plane wurtzite structures, the polarization of the probe beam is not an issue. However, with *M*-plane wurtzite nitrides, using an unpolarized probe beam or one that is polarized at an angle different from $\phi=0°$ or 90°, the resulting spectrum would be a weighted sum of the two spectra for $\phi=0°$ and 90°. From such an arbitrary resultant line shape, no meaningful EBS parameter can be extracted. In fact, a spectrum measured with $\phi=45°$ at 295 K (not shown here) gave a transition energy value equal to 3.483 eV, which is quite different from and even larger than the actual values of E_1 and E_2.

V. DISCUSSION

The XRD measurements show that the *M*-plane film is under biaxial compressive strain. Keeping this in mind and comparing the PR results with the calculated oscillator strength components in Fig. 4, we identify the lowest-energy PR feature seen for $\mathbf{E}\perp\mathbf{c}$ (i.e., $\mathbf{E}\|\mathbf{x}$) as the E_1 transition associated with a predominantly $|X\rangle$-like VB. The high energy PR feature, seen for $\mathbf{E}\|\mathbf{c}$ (i.e., $\mathbf{E}\|\mathbf{z}$), is identified as the E_2 transition associated with a predominantly $|Z\rangle$-like VB. The in-plane strain components ϵ_{xx} and ϵ_{zz} of the sample are those for which $E_1=3.498$ eV in Fig. 3(a) and $E_2=3.546$ eV in Fig. 3(b). The out-of-plane dilatation ϵ_{yy}, which is then obtained using Eq. (4), is matched to the experimental value $\epsilon_{yy}=0.29\%$ by varying the deformation potential D_5, resulting in $\epsilon_{xx}=-0.56\%$ and $\epsilon_{zz}=-0.31\%$.

For a Gaussian-broadened excitonic transition, the product of the amplitude and square of the broadening parameter ($a\gamma^2$) in Eq. (8) is proportional to the oscillator strength.[25] For the *x*-polarized E_1 and *z*-polarized E_2 transitions, the parameters obtained are approximately the same. The calculated relative *x* and *z* components of the oscillator strength of the E_1 and E_2 transitions, respectively, are both about 0.97 for $\epsilon_{xx}=-0.56\%$ and $\epsilon_{zz}=-0.31\%$. These two facts together suggest that the theoretical result of Suzuki and Uenoyama,[14] which predicted $|\langle S|p_x|X\rangle|^2=|\langle S|p_z|Z\rangle|^2$, is correct.

It is instructive to compare the present situation with unstrained or compressively strained *C*-plane GaN ($\epsilon_{xx}=\epsilon_{yy}$) with regard to the polarization properties. In such cases, one expects to see two dominant transitions (A and B exciton) for $\mathbf{E}\perp\mathbf{c}$ and one dominant transition (C exciton) for $\mathbf{E}\|\mathbf{c}$.[22] In effect, a polarization-dependent effective band-gap change would occur with a value equal in magnitude to the difference between the lowest-energy A and the highest-energy C transition. However, to our best knowledge, this has never been observed experimentally, because it is difficult to get pure $\mathbf{E}\|\mathbf{c}$ polarization with a *C*-plane GaN film.[16,27] With an *M*-plane film, both pure $\mathbf{E}\perp\mathbf{c}$ and pure $\mathbf{E}\|\mathbf{c}$ polarizations are possible, but here we see only one PR feature for $\mathbf{E}\perp\mathbf{c}$. At the same time, the energies of the features for both $\mathbf{E}\|\mathbf{c}$ and $\mathbf{E}\perp\mathbf{c}$ are quite different from the ones expected for unstrained GaN. Thus, although a polarization-dependent effective band-gap change is in principle possible even in unstrained GaN, the energies together with the polarization properties of the PR features in the present sample can only be explained by including the effect of in-plane biaxial compressive strain. We therefore have direct experimental evidence for an *M*-plane strain-induced EBS modification in GaN. Note also that for unstrained GaN the effective band-gap change would involve the lowest- (A-exciton) and highest- (C-exciton) energy transitions, while here it involves the lowest- (E_1) and next-higher- (E_2) energy transition. Detection of the highest-energy E_3 transition involving the $|Y\rangle$-like VB [expected at 3.58 eV in our sample as identified by the black spot in Fig. 3(c)] is not possible with PR, since a significant $\mathbf{E}\|\mathbf{y}$ polarization is not achievable with an *M*-plane film. In a polarized PL study of *M*-plane GaN grown on $(1\bar{1}00)$ 6H-SiC, shifts in the emission-peak positions were also reported,[28] but the shift was not attributed to a strain-induced EBS modification.

Gil and Alemu[17] have also reported a theoretical study of the EBS modification due to biaxial strain in the *M* plane of GaN. They predicted that for large in-plane compressive strain with $\mathbf{E}\perp\mathbf{c}$ (i.e., $\mathbf{E}\|\mathbf{x}$) both the lowest-energy (A-

exciton, according to their nomenclature) and the highest-energy (C-exciton) transitions would have significant oscillator strength. Their result differs from both of our results, namely, the theoretical calculations and experimental observations, since we do not observe the high-energy feature for **E**⊥ **c**. However, it is likely that their choice of coordinates was different[6] so that their *M* plane would correspond to the *A* plane in our case, which might be the cause for this discrepancy.

VI. SUMMARY

We have provided experimental evidence for the modification of the EBS of GaN due to biaxial strain in the *M* plane. We identified the PR features seen in the *M*-plane GaN sample for the two orthogonal polarizations **E**⊥ **c** and **E**‖**c** by comparing them with **k**·**p** EBS calculations. Their origin and the observed polarization properties were shown to be related to a modification of the VB of GaN due to in-plane compressive strain in the *M* plane. By matching the spectroscopically estimated strain to the value obtained from XRD measurements, we determined the deformation potential D_5 of GaN. The experimental results also support some of the earlier theoretical predictions regarding the influence of *M*-plane strain on the EBS of GaN. These results demonstrate the importance of the use of a properly polarized probe beam for postgrowth PR characterization of *M*-plane nitride layers.

ACKNOWLEDGMENTS

The authors would like to acknowledge the support of M. Ramsteiner, A. Thamm, U. Jahn, and L. Schrottke during the course of this work.

*Electronic address: htg@pdi-berlin.de

[1] F. Bernardini, V. Fiorentini, and D. Vanderbilt, Phys. Rev. B **56**, R10 024 (1997); F. Bernardini and V. Fiorentini, *ibid.* **57**, R9427 (1998); V. Fiorentini, F. Bernardini, F. Della Sala, A. Di Carlo, and P. Lugli, *ibid.* **60**, 8849 (1999); F. Bernardini, V. Fiorentini, and D. Vanderbilt, *ibid.* **63**, 193 201 (2001).

[2] T. Deguchi, K. Sekiguchi, A. Nakamura, T. Sota, R. Matsuo, S. Chichibu, and S. Nakamura, Jpn. J. Appl. Phys., Part 2 **38**, L914 (1999).

[3] P. Waltereit, O. Brandt, M. Ramsteiner, R. Uecker, P. Reiche, and K. H. Ploog, J. Cryst. Growth **218**, 143 (2000).

[4] P. Waltereit, O. Brandt, A. Trampert, H. T. Grahn, J. Menniger, M. Ramsteiner, M. Reiche, and K. H. Ploog, Nature (London) **406**, 865 (2000).

[5] *Group III Nitride Semiconductor Compounds*, edited by B. Gil (Clarendon, Oxford, 1998).

[6] A. Alemu, B. Gil, M. Julier, and S. Nakamura, Phys. Rev. B **57**, 3761 (1998).

[7] K. Domen, K. Horino, A. Kuramata, and T. Tanahashi, Appl. Phys. Lett. **71**, 1996 (1997).

[8] A. Niwa, T. Ohtoshi, and T. Kuroda, Appl. Phys. Lett. **70**, 2159 (1997).

[9] A. Thamm, O. Brandt, A. Trampert, and K. H. Ploog, Phys. Status Solidi A **180**, 73 (2000).

[10] F. H. Pollak, in *Group III Nitride Semiconductor Compounds*, edited by B. Gil (Clarendon, Oxford, 1998).

[11] G. L. Bir and G. E. Pikus, *Symmetry and Strain Induced Effects in Semiconductors* (Wiley, New York, 1974).

[12] M. Suzuki, T. Uenoyama, and A. Yanase, Phys. Rev. B **52**, 8132 (1995).

[13] K. Torii, T. Deguchi, T. Sota, K. Suzuki, S. Chichibu, and S. Nakamura, Phys. Rev. B **60**, 4723 (1999).

[14] M. Suzuki and T. Uenoyama, Jpn. J. Appl. Phys., Part 1 **35**, 543 (1996).

[15] A. Polian, M. Grimsditch, and I. Grzegory, J. Appl. Phys. **79**, 3343 (1996).

[16] A. Shikanai, T. Azuhata, T. Sota, S. Chichibu, A. Kuramata, K. Horino, and S. Nakamura, J. Appl. Phys. **81**, 417 (1997).

[17] B. Gil and A. Alemu, Phys. Rev. B **56**, 12 446 (1997).

[18] M. Suzuki and T. Uenoyama, Jpn. J. Appl. Phys., Part 1 **35**, 1420 (1996).

[19] W. Shan, A. J. Fischer, S. J. Hwang, B. D. Little, R. J. Hauenstein, X. C. Xie, J. J. Song, D. S. Kim, B. Goldberg, R. Horning, S. Krishnakutty, W. G. Perry, M. D. Bremser, and R. F. Davis, J. Appl. Phys. **83**, 455 (1998).

[20] A. A. Yamaguchi, Y. Mochizuki, C. Sasaoka, A. Kimura, M. Nido, and A. Usui, Appl. Phys. Lett. **71**, 374 (1997).

[21] T. Ohtoshi, A. Niwa, and T. Kuroda, J. Appl. Phys. **82**, 1518 (1997).

[22] B. Gil, F. Hamdani, and H. Morkoç, Phys. Rev. B **54**, 7678 (1996).

[23] B. Gil and O. Briot, Phys. Rev. B **55**, 2530 (1997).

[24] D. E. Aspnes, Surf. Sci. **37**, 418 (1973).

[25] S. Ghosh and H. T. Grahn, J. Appl. Phys. **90**, 500 (2001).

[26] O. J. Glembocki and B. V. Shanabrook, Superlattices Microstruct. **3**, 235 (1987).

[27] A. J. Fischer, W. Shan, J. J. Song, Y. C. Chang, R. Horning, and B. Goldenberg, Appl. Phys. Lett. **71**, 1981 (1997).

[28] K. Domen, K. Horino, A. Kuramata, and T. Tanahashi, Appl. Phys. Lett. **70**, 987 (1997).